

**DEUTSCHES ELEKTRONEN – SYNCHROTRON**

DESY 93-022  
UdeM-LPN-TH138  
February 1993



**CKM Parameter Fits,  
the  $B_s^0 - \overline{B}_s^0$  Mixing Ratio  $x_s$   
and CP-Violating Phases in  $B$  Decays**

A. Ali

*Deutsches Elektronen-Synchrotron DESY, Hamburg*

D. London

*Laboratoire de Physique Nucléaire, Université de Montréal, Québec, Canada*

ISSN 0418-9833

**NOTKESTRASSE 85 · D - 2000 HAMBURG 52**

DESY behält sich alle Rechte für den Fall der Schutzrechtserteilung und für die wirtschaftliche Verwertung der in diesem Bericht enthaltenen Informationen vor.

DESY reserves all rights for commercial use of information included in this report, especially in case of filing application for or grant of patents.

To be sure that your preprints are promptly included in the  
HIGH ENERGY PHYSICS INDEX,  
send them to (if possible by air mail):

**DESY**  
**Bibliothek**  
**Notkestraße 85**  
**W-2000 Hamburg 52**  
**Germany**

**DESY-IfH**  
**Bibliothek**  
**Platanenallee 6**  
**O-1615 Zeuthen**  
**Germany**

## 1 Introduction

In the Standard Model (SM) [1], fermions get their masses through Yukawa couplings involving a Higgs doublet field. For the quarks, the gauge- and mass-eigenstates are not the same, leading to intergenerational couplings in the weak charged-current interactions. These flavour non-diagonal couplings are described by the unitary Cabibbo-Kobayashi-Maskawa (CKM) matrix [2]. The CKM matrix is one of the few aspects of the SM which remains to be fully tested. The primary aim of experiments in  $B$  physics is to determine five of the nine CKM matrix elements, which can be measured in the charged current (CC) decays and in flavour changing neutral current (FCNC) processes. The CKM matrix elements in question are  $V_{ib}$ ,  $i = u, c$ , and those involving the  $t$ -quark,  $V_{tj}$ ,  $j = d, s, b$ . Knowledge of these matrix elements would determine the CKM parameters completely, hence also the CKM phase and with it all the CP-asymmetries in the quark sector. High-precision determinations of all CKM matrix elements may reveal some inconsistencies, and give us some clue as to the new physics which inevitably lies beyond the SM.

The aim of this article is to give the profile of the CKM matrix elements, in particular the CKM unitarity triangle, which the present measurements allow to be drawn, given the various input uncertainties. In updating the CKM matrix elements, we make use of the Wolfenstein parametrization [3]. The fits presented here differ from those given by us in ref. [4], which were based on the then current values of  $|V_{cb}|$  and  $|V_{ub}|$  [6], and the measured values of  $x_d$  ( $B_d^0$ - $\bar{B}_d^0$  mixing) and  $|\epsilon|$  (CP violation in the  $K$  sector). Since then, several experimental and theoretical numbers have changed and we take into account this evolution in the present update. These include the current averaged  $B$ -hadron lifetime,  $\tau_B = 1.36 \pm 0.04 \pm 0.06$  psec [5]<sup>2</sup>, which is significantly higher than the value used in ref. [4],  $\tau_B = 1.23 \pm 0.06$  psec, and the value of the CKM matrix element  $|V_{ub}|$ , whose present value [7],  $|V_{ub}/V_{cb}| = 0.08 \pm 0.02$ , is considerably lower than the one used in our earlier analysis [4],  $|V_{ub}/V_{cb}| = 0.14 \pm 0.05$ . On the theoretical side, the next-to-leading order QCD correction to the effective  $|\Delta B| = 2$  Hamiltonian gives  $\eta_B = 0.55$  [8], which is significantly lower than the earlier leading order result  $\eta_B = 0.85$  [9], and has some impact on the allowed range of the CKM parameters, using  $x_d$  in the fits as input. In view of this, we give here an update of our CKM fits.

We also show, to emphasize the role of  $x_d$ , the constraints that the possible measurement of the quantity  $x_d$ , or, equivalently, the ratio  $x_d/x_s$ , would have on the CKM parameters. Since the ratio  $x_d/x_s$  is independent of the top quark mass and the QCD corrections, and the dependence on other parameters is also greatly reduced, the measurement of  $x_d$  would have a significant impact on the CKM phenomenology. We give here our estimates for  $x_d$  in the SM context, which is expected to be  $x_d = O(10)$ , and review briefly the present (time-integrated) measurements of this quantity.

Having done the CKM fits, it is an easy matter to calculate the allowed ranges for the <sup>2</sup>This number takes into account the new LEP average and has actually been taken from a recent talk by M. Danilov at DESY.

## CKM Parameter Fits, the $B_s^0$ - $\bar{B}_s^0$ Mixing Ratio $x_s$ and CP-Violating Phases in $B$ Decays<sup>1</sup>

A. Ali

Deutsches Elektronen Synchrotron DESY  
Hamburg, Germany

D. London

Laboratoire de physique nucléaire, Université de Montréal  
C.P. 6128, Montréal, Québec, Canada H3C 3J7

### Abstract

We review and update constraints on the parameters of the flavour mixing matrix ( $V_{CKM}$ ) in the Standard Model. In performing these fits, we use inputs from the measurements of  $|\epsilon|$ , the CP-violating parameter in  $K$  decays,  $x_d = (\Delta M)/\Gamma$ , the mixing parameter in  $B_d^0$ - $\bar{B}_d^0$  mixing, and the present measurements of the matrix elements  $|V_{cb}|$  and  $|V_{ub}|$ . We take into account the next-to-leading order QCD results in our analysis, wherever available, and incorporate results stemming from the ongoing lattice calculations of the  $B$ -meson coupling constants, which predict a value  $f_{B_d} = 200 \pm 30$  MeV, though for the sake of comparison we also show the CKM fits for smaller values of  $f_{B_d}$ . We use the updated CKM matrix to predict the mixing ratio  $x_d$ , relevant for  $B^0$ - $\bar{B}^0$  mixing, and the phases in the CKM unitarity triangle,  $\sin 2\alpha$ ,  $\sin 2\beta$  and  $\sin 2\gamma$ , which determine the CP-violating asymmetries in  $B$ -decays. The importance of measuring the ratio  $x_d$  in restricting the allowed values of the CKM parameters is emphasized.

<sup>1</sup>to be published in the Proceedings of the ECFA Workshop on the Physics of a  $B$  Meson Factory, Editors: R.Alekसान and A.Ali (1993).

CP-violating phases that will be measured in  $B$  decays. Using the CKM unitarity triangle, these phases, denoted by  $\sin 2\beta$ ,  $\sin 2\alpha$  and  $\sin 2\gamma$ , measure the angles of this triangle (see Fig. 1). Of course, in the SM, all these phases are related to the CKM phase. They can be measured directly through asymmetries in the decays  $B \rightarrow J/\psi + K_S$ ,  $B \rightarrow \pi^+ \pi^-$ , and in  $B_c \rightarrow \rho K_S$ , respectively. Indirectly, one could also determine them from the precision measurements of the three sides of the unitarity triangle in CC and FCNC process in the  $B$  system. We also present the allowed domains for two of the angles, ( $\sin 2\beta$ ,  $\sin 2\alpha$ ).

We start in section 2 with the updates of the CKM fits. In section 3, we give our SM estimates for  $x$ , and discuss how a measurement of  $x$ , will help pin down the CKM matrix elements. We also update the time-integrated measurements of  $B^0\text{-}\bar{B}^0$  mixing in this section. The general issues involved in a time-dependent measurement of  $x$ , and the experimental prospects for measuring  $x$ , have been discussed at length by us recently in ref. [4] and are not dealt with here. In section 4, we give our estimates for the allowed domains for the CP-violating phases  $\sin 2\beta$ ,  $\sin 2\alpha$  and  $\sin 2\gamma$ , including the correlations between  $\sin 2\beta$  and  $\sin 2\alpha$ . We give a summary in Section 5.

## 2 An Update of the CKM Matrix

### 2.1 The CKM matrix parameters

For 3 generations, the CKM matrix can be described by 3 angles and one complex phase. It was noticed some time ago by Wolfenstein [3] that the elements of this matrix exhibited a hierarchy in terms of  $\lambda$ , the Cabibbo angle. In this parametrization the CKM matrix can be written approximately as

$$V_{CKM} \simeq \begin{pmatrix} 1 - \frac{1}{2}\lambda^2 & \lambda & A\lambda^3(\rho - i\eta) \\ -\lambda & 1 - \frac{1}{2}\lambda^2 - iA^2\lambda^4\eta & A\lambda^2 \\ A\lambda^3(1 - \rho - i\eta) & -A\lambda^2 & 1 \end{pmatrix}. \quad (1)$$

For a detailed discussion about the model dependence and methods of extraction of the CKM parameters  $\lambda$ ,  $A$ ,  $\rho$ , and  $\eta$ , we refer the reader to our paper [4]. Here, we shall restrict ourselves to specifying the main input, pointing out the significant changes since we presented our earlier fits.

We recall that  $|V_{us}|$  has been extracted with good accuracy from  $K \rightarrow \pi e \nu$  and hyperon decays [6] to be

$$|V_{us}| = \lambda = 0.2205 \pm 0.0018. \quad (2)$$

This agrees quite well with the determination of  $V_{ud} \simeq 1 - \frac{1}{2}\lambda^2$  from  $\beta$ -decay:

$$|V_{ud}| = 0.9744 \pm 0.0010. \quad (3)$$

The parameter  $A$  is related to the CKM matrix element  $V_{cb}$ , which can be obtained from semileptonic decays of  $B$  mesons. We shall restrict ourselves to the methods based on

the heavy-quark effective theory (HQET). In the heavy quark limit it has been observed that all hadronic form factors can be expressed in terms of a single function, the Isgur-Wise function [10]. It has been shown that the HQET-based method works best for  $B \rightarrow D^* l \nu$  decays, since these decays are unaffected by  $1/m_b$  corrections [11,12,13]. Furthermore, the QCD corrections calculated in HQET turn out to be small [13]. This method has been used by both the ARGUS and CLEO collaboration [14].

Following ref. [15], the measured branching ratios for the charged and neutral  $D^*$  modes,  $B \rightarrow D^{*+} l \nu$  and  $B \rightarrow D^{*0} l \nu$ , the lepton energy spectrum, which is consistent with a linear extrapolation of the Isgur-Wise function to the symmetry point, and the present value of the  $B$  lifetime,

$$\tau_B = (1.36 \pm 0.04 \pm 0.06) \times 10^{-12} \text{ sec}, \quad (4)$$

can be used to extract the value of  $|V_{cb}|$ . The ARGUS analysis gives the following value for  $|V_{cb}|$ :

$$|V_{cb}| = 0.044 \pm 0.006, \quad (5)$$

where we have updated the value for  $\tau_B$  used by them and have added the errors quoted by them in quadrature. The dependence on the matrix element  $|V_{cb}|$  on the assumed parametrization of the Isgur-Wise function can be found in ref. [15]. For the purposes of the fits which follow, we shall use the value of the CKM parameter  $A$  obtained from the above HQET-based method:

$$A = 0.90 \pm 0.12. \quad (6)$$

Though the experimental numbers for  $\tau_B$  and the exclusive semileptonic branching ratios for the decay modes,  $D^*$  modes,  $B \rightarrow D^{*+} l \nu$  and  $B \rightarrow D^{*0} l \nu$ , have changed, they have conspired in such a way that the determination of  $A$  remains unchanged from its value used in ref. [4]. The other two CKM parameters  $\rho$  and  $\eta$  are constrained by the measurements of  $|V_{ub}/V_{cb}|$ ,  $|\epsilon|$  (the CP-violating parameter in the kaon system),  $x_d$  ( $B_d^0\text{-}\bar{B}_d^0$  mixing) and (in principle)  $\epsilon'/\epsilon$  ( $\Delta S = 1$  CP-violation in the kaon system). We shall not discuss the constraints from  $\epsilon'/\epsilon$ , due to the various experimental and theoretical uncertainties surrounding it at present, but take up the rest in turn and present fits in which the allowed region of  $\rho$  and  $\eta$  is shown.

First of all,  $|V_{ub}/V_{cb}|$  can be obtained by looking at the endpoint of the inclusive lepton spectrum in semileptonic  $B$  decays. The older results from ARGUS and CLEO and their model dependent translation in terms of the parameter  $|V_{ub}/V_{cb}|$  can be found in ref. [4]. These results were interpreted to yield [4]:

$$\frac{|V_{ub}|}{|V_{cb}|} = 0.14 \pm 0.05. \quad (7)$$

However, as noted already in the introduction, there has been a significant scaling down of this ratio since the Dallas conference [14]. The present average of this ratio, based on the recent analysis of the ARGUS and CLEO data, is [7]:

$$\frac{|V_{ub}|}{|V_{cb}|} = 0.08 \pm 0.02. \quad (8)$$

This number is obtained using the model of Altarelli et. al. [16], and we take it as a realistic estimate of the above ratio. This gives

$$\sqrt{\rho^2 + \eta^2} = 0.36 \pm 0.09. \quad (9)$$

The smaller value of  $|V_{cb}/V_{cs}|$  has a considerable effect on the allowed domains for the parameters  $(\rho, \eta)$ , given below.

The experimental value of  $|\epsilon|$  is [6]

$$|\epsilon| = (2.26 \pm 0.02) \times 10^{-3}. \quad (10)$$

Theoretically,  $|\epsilon|$  is essentially proportional to the imaginary part of the box diagram for  $K^0 \bar{K}^0$  mixing and is given by [9]

$$|\epsilon| = \frac{G_F^2 V_K^2 M_K M_W^2}{6\sqrt{2}\pi^2 \Delta M_K} B_K (A^2 \lambda^6 \eta) (y_c \{\eta_{ct} f_3(y_c, y_t) - \eta_{cc}\} + \eta_{tt} y_t f_2(y_t) A^2 \lambda^4 (1 - \rho)). \quad (11)$$

Here, the  $\eta_i$  are QCD correction factors,  $\eta_{cc} \simeq 0.82$ ,  $\eta_{tt} \simeq 0.62$ ,  $\eta_{ct} \simeq 0.35$  for  $\Lambda_{QCD} = 200$  MeV [17],  $y_i \equiv m_i^2/M_W^2$ , and the functions  $f_2$  and  $f_3$  are given by

$$f_2(x) = \frac{1}{4} + \frac{9}{4} \frac{1-x}{1-x} - \frac{3}{2} \frac{x^2 \ln x}{(1-x)^2} - \frac{3}{2} \frac{x^2 \ln x}{2(1-x)^3}, \quad (12)$$

$$f_3(x, y) = \ln \frac{y}{x} - \frac{3y}{4(1-y)} \left( 1 + \frac{y}{1-y} \ln y \right).$$

(The above form for  $f_3(x, y)$  is an approximation, obtained in the limit  $x \ll y$ . For the exact expression, see ref. [18].) One of the unknowns in Eq. 11 is the top quark mass. We shall use the range

$$100 \text{ GeV} \leq m_t \leq 180 \text{ GeV}. \quad (13)$$

which is consistent with the present CDF bounds from direct top searches [19], and the electroweak phenomenology predicting a range for  $m_t$  [20, 21, 22]. While the exact range of  $m_t$  depends on a number of details, in particular on value of  $\alpha_s$ , a recent analysis based on the combined LEP data gives [23]:

$$m_t = 148_{-26}^{+22} - {}_{-23}^{+19} (M_H = 175 \text{ V}) \text{ GeV} \quad (14)$$

with  $\alpha_s(M_Z^2) = 0.125 \pm 0.005 \pm 0.002(M_H)$ .

The final parameter in the expression for  $|\epsilon|$  is  $B_K$ , which represents our ignorance of the matrix element  $\langle K^0 | (\bar{d}\gamma^\mu(1-\gamma_5)s)^2 | \bar{K}^0 \rangle$ . The evaluation of this matrix element has been the subject of much work. The results are summarized in ref. [4]. Although the entire range of  $B_K$  is  $1/3 \leq B_K \leq 1$ , the  $1/N$  and lattice approaches are generally considered more reliable. For this reason, in what follows we shall take

$$B_K = 0.8 \pm 0.2. \quad (15)$$

which is the value used in ref. [4].

We now turn to  $B_d^0 \bar{B}_d^0$  mixing. The latest value of  $x_d$ , which is a measure of this mixing, is [24]

$$x_d = 0.67 \pm 0.10. \quad (16)$$

The mixing parameter  $x_d$  is calculated from the  $B_d^0 \bar{B}_d^0$  box diagram. Unlike the kaon system, where the contributions of both the  $c$ - and the  $t$ -quarks in the loop were important, this diagram is dominated by  $t$ -quark exchange:

$$\langle \Delta M \rangle_B = \frac{G_F^2}{\Gamma} M_W^2 M_B (f_{B_d}^2 B_{B_d}) \eta_B y_t f_2(y_t) |V_{td}^* V_{tb}|^2, \quad (17)$$

where, using Eq. 1,  $|V_{td}^* V_{tb}|^2 = A^2 \lambda^6 [(1-\rho)^2 + \eta^2]$ . Here,  $\eta_B$  is the QCD correction. In ref. [8], this correction is analyzed in great detail, including the effects of a heavy  $t$ -quark. They find that  $\eta_B$  depends sensitively on the definition of the  $t$ -quark mass, and that, strictly speaking, only the product  $\eta_B(y_t) f_2(y_t)$  is free of this dependence. In the fits presented here we use the value  $\eta_B = 0.55$ , following ref. [8].

For the  $B$  system, the hadronic uncertainty is given by  $f_{B_d}^2 B_{B_d}$ , analogous to  $B_K$  in the kaon system, except that in this case, also  $f_{B_d}$  is not measured. And, just like  $B_K$ , the evaluation of  $f_{B_d}^2 B_{B_d}$  has been the subject of much work, summarized in ref. [4]. Until very recently the scaling law,

$$f_B(m_B) \sqrt{m_B} = \text{constant}, \quad (18)$$

was thought to be valid for the  $B$  system. This led to rather small values for  $f_{B_d}^2 B_{B_d}$  in the range

$$100 \text{ MeV} \leq f_{B_d} \sqrt{B_{B_d}} \leq 170 \text{ MeV}. \quad (19)$$

However, recent lattice calculations have indicated that there are significant scaling violations. These have led to larger estimates for  $f_{B_d}^2 B_{B_d}$ , roughly in the range

$$200 \text{ MeV} \leq f_{B_d} \sqrt{B_{B_d}} \leq 300 \text{ MeV}. \quad (20)$$

We will therefore consider two ranges for  $f_{B_d}^2 B_{B_d}$ , corresponding approximately to the ranges in Eqs. 19 and 20:

$$(I): f_{B_d} \sqrt{B_{B_d}} = 135 \pm 25 \text{ MeV},$$

$$(II): f_{B_d} \sqrt{B_{B_d}} = 200 \pm 30 \text{ MeV} \quad (21)$$

The number quoted for the coupling constant ( $II$ ) has also been scaled down from the value  $f_{B_d} \sqrt{B_{B_d}} = 240 \pm 40$  MeV used in our previous analysis [4], following the advice of our lattice colleagues [25, 26].

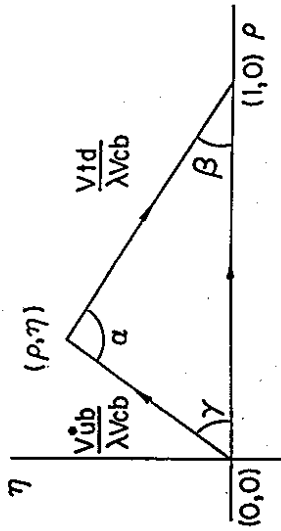


Figure 1: The unitarity triangle. The angles  $\alpha$ ,  $\beta$  and  $\gamma$  can be measured via CP violation in the  $B$  system.

## 2.2 The unitarity triangle

The information regarding the allowed region in  $\rho$ - $\eta$  space can be displayed quite elegantly using the so-called unitarity triangle. This is constructed as follows. Because the CKM matrix is unitary, one has the following relation:

$$V_{ud}V_{cb}^* + V_{td}V_{cb}^* + V_{td}V_{ub}^* = 0. \quad (22)$$

Using the form of the CKM matrix in Eq. 1, this can be recast as

$$\frac{V_{ub}^*}{\lambda V_{cb}} + \frac{V_{td}}{\lambda V_{cb}} = 1, \quad (23)$$

that is, a triangle relation in the complex plane (i.e.  $\rho$ - $\eta$  space). This is illustrated in Fig. 1. Thus, allowed values of  $\rho$  and  $\eta$  translate into allowed shapes of the unitarity triangle.

In order to find the allowed unitarity triangles, the computer program MINUIT was used in ref. [4] to fit the CKM parameters  $A$ ,  $\rho$  and  $\eta$  to the experimental values of  $|V_{cb}|$ ,  $|V_{ub}/V_{cb}|$ ,  $|e|$  and  $x_d$ . This fit is updated in this contribution and the results are shown in Fig. 2 and Fig. 3 for the coupling constant choices  $(I)$  and  $(II)$ , respectively. For the uncertainties in the hadronic matrix elements, we use the ranges for  $B_K$  and  $f_{B_s}^2 B_{B_s}$  defined in Eqs. 15 and 21. (Note that, strictly speaking, this is not correct – theoretical “errors” are not Gaussian. However, this method is not unreasonable, being quite similar to the practice of adding experimental statistical and systematic errors in quadrature.) Note that the graph for  $f_{B_s} \sqrt{B_{B_s}} = 135 \pm 25$  MeV and  $m_t = 100$  GeV is a poor fit of the data ( $\chi^2 = 1.97$ ). In all these graphs, the solid line has  $\chi^2 = \chi_{\min}^2 + 1$ . Note that,

$m_t$ (GeV)	$f_{B_s} \sqrt{B_{B_s}}$ (MeV)	$(\rho, \eta)$	$ V_{td}/V_{cb} ^2$	$\chi_{\min}^2$
100	$135 \pm 25$	$(-0.30, 0.25)$	0.085	1.97
140	$135 \pm 25$	$(-0.33, 0.18)$	0.087	0.32
180	$135 \pm 25$	$(-0.32, 0.16)$	0.086	0.03
100	$200 \pm 30$	$(-0.23, 0.30)$	0.078	0.15
140	$200 \pm 30$	$(-0.04, 0.34)$	0.058	0.30
180	$200 \pm 30$	$(0.23, 0.25)$	0.032	0.20

Table 1: The “best values” of the CKM parameters  $(\rho, \eta)$  and the ratio  $|V_{td}/V_{cb}|^2$ , obtained by a minimum  $\chi^2$  fit of the experimental data discussed in the text. Values of  $m_t$  and the coupling constant  $f_{B_s} \sqrt{B_{B_s}}$  are stated. The resulting minimum  $\chi^2$  values from the MINUIT fits are also given.

although many authors use this curve to represent “ $1\sigma$ ”, it is, in fact, only a 39% confidence level region [6]! For comparison, we include the dashed line, which is the 90% c.l. region ( $\chi^2 = \chi_{\min}^2 + 4.6$ ). It is clear that, as we pass from Fig. 2(a) to Fig. 3(c), the “most likely” unitarity triangles become more and more acute, as has already been pointed out [27]. However, it is also clear that there is a substantial overlap between the 90% c.l. regions of  $f_{B_s} \sqrt{B_{B_s}} = 135 \pm 25$  MeV and those with  $f_{B_s} \sqrt{B_{B_s}} = 200 \pm 30$  MeV. The “best values” of the parameters  $(\rho, \eta)$ , and the CKM matrix element ratio  $|V_{td}/V_{cb}|^2$  together with their  $\chi^2$ , are given in Table 1.

We remark that the range of  $\eta$  is well constrained by the very accurate measurement of  $|e|$ , and it depends only modestly on  $x_d$  (and hence  $f_{B_s}$ ), or as we are going to argue in the next section, on the ratio  $x_s/x_d$ . On the other hand,  $\rho$  is strongly affected by the  $x_d$  measurement, which in turn depends strongly on both  $m_t$  and  $f_{B_s}$ . It is therefore qualitatively clear that a good measurement of  $x_s$  (and hence  $x_s/x_d$ ) will be very effective in narrowing down the allowed range for  $\rho$ . We will return to a quantitative discussion of this point in the next section. It is also appropriate to point out that the pseudoscalar coupling constant  $f_D$ , has been measured recently via the purely leptonic decay  $D_s^\pm \rightarrow \mu^\pm \nu_\mu$ , by the WA75 collaboration, giving  $f_D = (232 \pm 45 \pm 20 \pm 48)$  MeV [28]. It is tempting to compare this measurement with a compilation based on lattice QCD calculations, which quotes for the same quantity [29]  $f_D = (180 \pm 25 \pm 30)$  MeV. So, whereas there are still substantial errors on both theoretical and experimental measurements, the two are consistent with each other.

## 3 $B_s^0$ - $\bar{B}_s^0$ Mixing

It is evident from Figs. 2-3 that there is, at present, a great deal of uncertainty in the shape of the unitarity triangle, mostly due to the uncertainty in the coupling constants but also

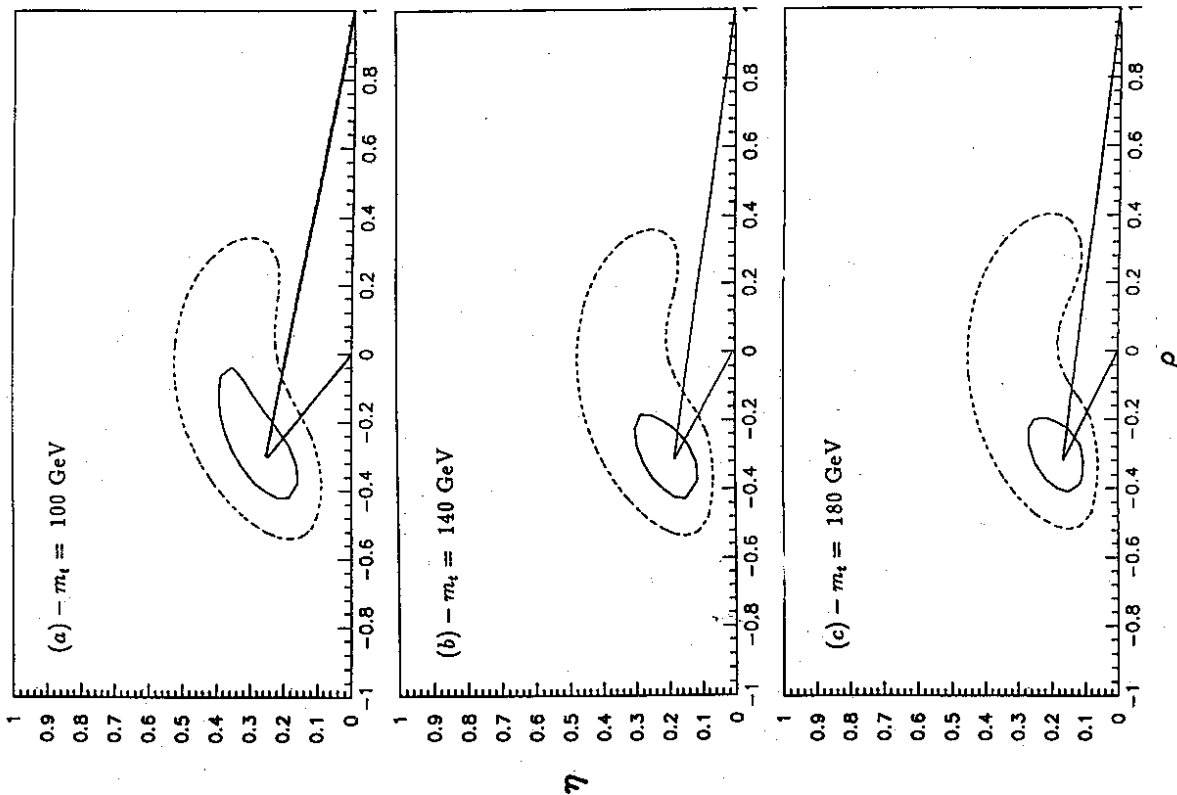


Figure 2: Allowed region in  $\rho$ - $\eta$  space for different values of the standard model parameters. Figs. (a)-(c) have  $f_{B_d}\sqrt{B_{B_d}} = 135 \pm 25$  MeV, with  $m_t = 100, 140$  and  $180$  GeV, respectively. The solid line represents the region with  $\chi^2 = \chi_{\min}^2 + 1$ ; the dashed line denotes the 90% c.l. region. The triangles show the best fit.

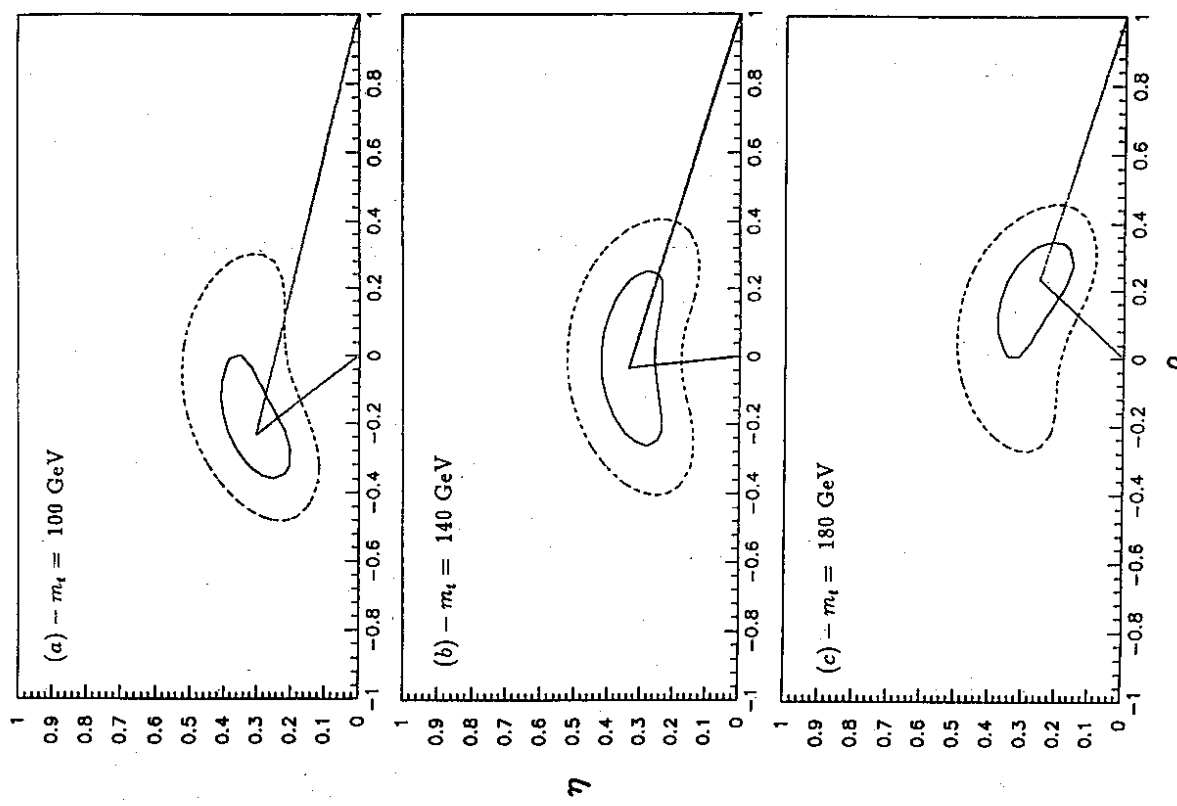


Figure 3: Allowed region in  $\rho$ - $\eta$  space for different values of the standard model parameters. Figs. (a)-(c) have  $f_{B_d}\sqrt{B_{B_d}} = 200 \pm 30$  MeV, with  $m_t = 100, 140$  and  $180$  GeV, respectively. The solid line represents the region with  $\chi^2 = \chi_{\min}^2 + 1$ ; the dashed line denotes the 90% c.l. region. The triangles show the best fit.

to some extent due to the imprecise value of  $m_t$ . If we wish to test the CKM matrix as the explanation for CP violation, we will need much more information. Ideally, we should measure enough angles and sides to overconstrain the unitarity triangle of Fig. 1. How can we do this? First of all, the angles  $\alpha$ ,  $\beta$  and  $\gamma$  can be measured via CP violating rate asymmetries in the  $B$  system [30,31]. The angle  $\sin 2\alpha$  is measured in the decays  $B_d^0(B_s^0) \rightarrow \pi^+ \pi^-$ ,  $\sin 2\beta$  is measured through  $B_d^0(B_s^0) \rightarrow J/\psi K_S$ , and  $\sin 2\gamma$  is measured in  $B_d^0(B_s^0) \rightarrow \rho K_S$  [32]. Obviously, if all three angles were obtained in this way with enough accuracy, this would suffice to ascertain whether or not the unitarity triangle closes, i.e. whether or not CP violation can be explained via the CKM matrix. However, it appears to be extremely difficult, at least for the first generation of  $B$ -factories, to measure the angle  $\gamma$ . It is therefore necessary to combine the measurements of  $\alpha$  and  $\beta$  with a measurement of one of the sides ( $|V_{ub}/\lambda V_{cb}|$  or  $|V_{td}/\lambda V_{cb}|$ ). Unfortunately, there is still quite a bit of uncertainty, mostly theoretical, in  $|V_{ub}/\lambda V_{cb}|$ . Furthermore, although one can extract a value of  $|V_{td}|$  from a measurement of  $x_d$ , the unknown  $t$ -quark mass and the considerable uncertainty in  $f_{B_d}^2 B_{B_d}$  (Eqs. 19,20) will lead to a rather imprecise value for this quantity.

There are several possible resolutions to this problem. First of all, it may be possible to measure the parameter  $f_{B_d}$ , using isospin symmetry, via the CC decay  $B_u^+ \rightarrow \tau^+ \nu_\tau$ . With  $|V_{cb}|/|V_{cb}| = 0.08 \pm 0.02$  and  $f_{B_d} = 200 \pm 30$  MeV, used here, one gets a branching ratio  $BR(B_u^+ \rightarrow \tau^+ \nu_\tau) = (0.5-2.4) \times 10^{-4}$ , which lies in the range of the future LEP and asymmetric B factory experiments. Along the same lines, the prospects of measuring  $(f_{B_d}, f_{B_s})$  in the FCNC leptonic and photonic decays of  $B_d^0$  and  $B_s^0$  hadrons,  $(B_d^0, B_s^0) \rightarrow \tau^+ \tau^-$ ,  $(B_d^0, B_s^0) \rightarrow \gamma \gamma$  in future  $B$  physics facilities are not entirely dismal. Their branching ratios (assuming  $f_{B_d} = 200$  MeV and  $m_t = 150$  GeV) have been estimated as  $BR(B_d^0 \rightarrow \tau^+ \tau^-) = 3.6 \times 10^{-7}$  and  $BR(B_d^0 \rightarrow \gamma \gamma) = 2 \times 10^{-8}$  [33]. Our "best estimates" for the coupling constant ratio  $|V_{td}/V_{cb}|^2$ , given in Table 1, would then put the corresponding branching ratios for the  $B_d^0$ -mesons typically a factor 20 below those of  $B_s^0$ . We are hopeful that the uncertainty on  $f_{B_d}$  and  $f_{B_s}$  will be much reduced by their direct measurements in future experiments.

Secondly, the error on  $|V_{ub}/\lambda V_{cb}|$  could perhaps be reduced by experimentally ruling out certain models. A third, perhaps more interesting, possibility is to use rare  $B$ -decays involving the transitions  $b \rightarrow s$  and  $b \rightarrow d$ . Of these, the CKM-suppressed radiative decays  $B \rightarrow X_d + \gamma$  (and  $B \rightarrow \rho + \gamma$ , ...) as well as the FCNC semileptonic decays  $B \rightarrow X_d + (\ell^+ \ell^-)$  (and  $B \rightarrow (\pi, \rho, A_1, \dots)(\ell^+ \ell^-)$ ) are particularly useful since they all measure the CKM matrix element  $|V_{td}|$ . The inclusive rates depend only on  $m_t$  while the exclusive rates depend also on form factors. However, it can be shown that the relative rates satisfy the following relations (up to small  $SU(3)$ -breaking effects denoted by  $\delta_i$ ) [34]:

$$\Gamma(b \rightarrow d + \gamma)/\Gamma(b \rightarrow s + \gamma) = \frac{|V_{td}|^2}{|V_{ts}|^2} (1 + \delta_1), \quad (24)$$

$$\Gamma(b \rightarrow d + \ell \bar{\ell})/\Gamma(b \rightarrow s + \ell \bar{\ell}) = \frac{|V_{td}|^2}{|V_{ts}|^2} (1 + \delta_2). \quad (25)$$

Similar relations also apply to the ratios of the exclusive rare decays, for example,  $\Gamma(B \rightarrow \rho + \gamma)/\Gamma(B \rightarrow K^* + \gamma)$  and  $\Gamma(B \rightarrow \rho + \ell \bar{\ell})/\Gamma(B \rightarrow K^* + \ell \bar{\ell})$  ( $\ell = e, \mu, \tau, \nu$ ). The estimated rates are such that some should be measurable in a first generation  $B$ -factory with  $O(10^7)$  events [33].

Another possibility, which is the one we will emphasize, is to use the information from  $x_s$ , the  $B_s^0, \bar{B}_s^0$  mixing parameter.

### 3.1 $x_s$ and the unitarity triangle

Mixing in the  $B_s^0, \bar{B}_s^0$  system follows quite closely that of the  $B_d^0, \bar{B}_d^0$  system. The  $B_s^0, \bar{B}_s^0$  box diagram is again dominated by  $t$ -quark exchange, and the mixing parameter  $x_s$  is given by a formula analogous to that of Eq. 17:

$$x_s \equiv \frac{(\Delta M)_{B_s}}{\Gamma_{B_s}} = \frac{G_F^2}{\Gamma_{B_s}} M_W^2 M_{B_s} (f_{B_s}^2 B_{B_s}) \eta_{B_s} y_2(y_s) |V_{ts}^* V_{tb}|^2. \quad (26)$$

Using the fact that  $|V_{cb}| = |V_{cs}|$  (Eq. 1), it is clear that one of the sides of the unitarity triangle,  $|V_{td}/\lambda V_{cb}|$ , can be obtained from the ratio of  $x_d$  and  $x_s$ :

$$\frac{x_d}{x_s} = \frac{\tau_{B_d} \eta_{B_d} M_{B_d} (f_{B_d}^2 B_{B_d})}{\tau_{B_s} \eta_{B_s} M_{B_s} (f_{B_s}^2 B_{B_s})} \frac{|V_{td}|^2}{|V_{ts}|^2}. \quad (27)$$

All dependence on the  $t$ -quark mass drops out, and we are left with the square of the ratio of CKM matrix elements, multiplied by a factor which reflects  $SU(3)_{\text{flavour}}$  breaking effects. The only real uncertainty in this factor is the ratio of hadronic uncertainties - the other quantities will be either calculated or measured. Whether or not  $x_s$  can be used to help constrain the unitarity triangle will depend crucially on the theoretical status of the ratio  $f_{B_d}^2 B_{B_d}/f_{B_s}^2 B_{B_s}$ .

Lattice calculations indicate that the ratio  $f_{B_d}/f_{B_s}$  could be calculated much more accurately than either of  $f_{B_d}$  or  $f_{B_s}$ , due to the cancellation of some systematic uncertainties. For example, ref. [35] gives

$$\begin{aligned} f_{B_d} &= 188-246 \text{ MeV}, \\ f_{B_s} &= 204-241 \text{ MeV}. \end{aligned} \quad (28)$$

Along the same lines, Abada et al. [36] quote  $f_{B_s}/f_{B_d} = 1.06 \pm 0.04$ ; a recent average over a number of lattice calculations gives  $f_{B_s}/f_{B_d} = 1.08 \pm 0.06$  [26], with the quantity actually appearing in the ratio  $x_s/x_d$  having been estimated as [37]:

$$\frac{f_{B_s}^2 B_{B_s}}{f_{B_d}^2 B_{B_d}} = 1.19 \pm 0.10 \quad (29)$$



It is not clear whether the error on this ratio will remain smaller than the error on either  $f_{B_s}$  or  $f_{B_d}$ . This is the crucial point – if  $f_{B_s}$  can be calculated as accurately as  $f_{B_s}/f_{B_d}$ , then the measurement of  $x$ , will not help in extracting the CKM matrix element  $V_{td}$  with more precision, assuming that the  $t$ -quark mass is known. On the other hand, if the calculation of  $f_{B_s}/f_{B_d}$  is more accurate than that of  $f_{B_d}$ , or if the  $t$ -quark mass is still unknown (which seems unlikely), then a measurement of  $B_s^0\text{-}\bar{B}_s^0$  mixing will allow a more accurate measurement of  $|V_{td}/\lambda V_{cb}|$ , and will be an important further test of the unitarity triangle. (It should be noted that, even if it turns out that  $x$ , is not as useful as is hoped for constraining the unitarity triangle in the above manner, its value is in any case necessary to obtain the angle  $\gamma$  via CP violation in  $B_s$  decays.)

Having motivated the necessity for measuring  $x$ , we will now turn to an estimate of its size in the standard model. We shall not entertain scenarios beyond the standard model, referring instead to our earlier paper [4].

### 3.2 Standard model prediction for $x$ ,

The SM expression for  $x$ , is given in Eq. 26. Using Eq. 1 to substitute for  $V_{td}^*V_{cb}$ , we obtain

$$x = \tau_{B_s} \frac{G_F^2}{6\pi^2} M_W^2 M_{B_s} (f_{B_s}^2 B_{B_s}) \eta_{B_s} A^4 y_t f_2(y_t). \quad (30)$$

The main uncertainties in this equation are again the  $t$ -quark mass and  $f_{B_s}^2 B_{B_s}$ . The lifetime of the  $B_s$  meson has now been measured at LEP. We give below the LEP average for the  $B_s^0$  and  $B_s^{\pm}$  lifetimes [14]:

$$\begin{aligned} \tau_{B_s^0} &= (1.05 \pm 0.32) \times 10^{-12} \text{ sec} \\ \tau_{B_s^{\pm}} &= (1.46 \pm 0.19) \times 10^{-12} \text{ sec} \end{aligned} \quad (31)$$

Within the measurement errors, both these values are consistent with the averaged value of  $\tau_B$  used in the previous section. There is no measurement yet for the mass of the  $B_s^0$  mesons. We will assume that the  $B_s^0\text{-}B_s$  mass difference is 100 MeV [38]. We will also take the QCD correction  $\eta_{B_s}$  to be equal to its  $B_d$  counterpart, i.e.,  $\eta_{B_s} = 0.55$ . Using the value for  $A$ , Eq. 6, we obtain

$$x = (153 \pm 26) \frac{f_{B_s}^2 B_{B_s}}{(1 \text{ GeV})^2} y_t f_2(y_t). \quad (32)$$

For 89 GeV  $\leq m_t \leq 182$  GeV, the function  $y_t f_2(y_t)$  is in the range 0.88-2.72, and is equal to 2.03 for the central value of  $m_t$ , 150 GeV. As for  $f_{B_s}^2 B_{B_s}$ , as mentioned earlier, there is some controversy regarding its value. We will therefore consider two ranges for  $f_{B_s}^2 B_{B_s}$ :

$$\begin{aligned} (I) : \quad f_{B_s} \sqrt{B_{B_s}} &= 180 \pm 35 \text{ MeV}, \\ (II) : \quad f_{B_s} \sqrt{B_{B_s}} &= 225 \pm 25 \text{ MeV}. \end{aligned} \quad (33)$$

This leads to

$$\begin{aligned} (I) : \quad x &= (5.0 \pm 1.6) y_t f_2(y_t), \\ (II) : \quad x &= (7.8 \pm 1.8) y_t f_2(y_t), \end{aligned} \quad (34)$$

which gives “ $1\sigma$ ” lower limits

$$\begin{aligned} (I) : \quad x &> 3.0, \\ (II) : \quad x &> 5.2. \end{aligned} \quad (35)$$

The “central values” (taking  $m_t = 150$  GeV) are

$$\begin{aligned} (I) : \quad x &= 10.0, \\ (II) : \quad x &= 15.8. \end{aligned} \quad (36)$$

The standard model therefore predicts very large values for  $x$ . This is to be expected since, from Eq. 27, one has  $x/x_d = |V_{td}/V_{ts}|^2$ , which in our estimates lies between 11.5 and 31, apart from  $SU(3)_{\text{flavour}}$  breaking effects. Using the central value for  $x_d = 0.67$ , this gives  $x \simeq (8\text{-}21)$ . Due to these large values, time-dependent measurements are necessary to obtain  $x$ .

### 3.3 CKM fits imposing constraints from $x$ ,

In the previous section we have given our CKM fits, using the measured value of  $x_d$  and its SM analysis, which depends on  $m_t$ , the coupling constant product  $f_{B_s}^2 B_{B_s}$ , and the QCD correction factor  $\eta_B$ . These fits show that the allowed region in  $\rho\text{-}\eta$  is enormous, reflecting the large uncertainties in some of the input parameters. We have also argued that much of the uncertainty in the allowed region would disappear if, instead of  $x_d$ , one used the ratio  $x/x_d$  to constrain the CKM parameters. The main point is that if this ratio were measured then one could restrict the allowed value of  $\rho$ . Unfortunately,  $x$ , has not been measured. However, the point can be illustrated by assuming a value for  $x$ , based on our SM estimates of this quantity in the previous section. We assume, for the sake of the CKM fits in this section,

$$x = 15.0 \pm 3.0. \quad (37)$$

We now impose the constraints from this hypothetical measurement of  $x$ , together with the measured value for  $x_d$ , and the lattice QCD estimates of the coupling constant product (Eq. 29). The other constraints from the measured values of  $|\epsilon|$ ,  $|V_{cb}|$  and  $|V_{ub}|$ , which we have employed earlier, remain unchanged in these fits. The resulting CKM fits are shown in Figs. 4, for the three assumed values of  $m_t = 100, 140$  and 180 GeV. Note that the allowed regions in the  $(\rho, \eta)$  for the three choices of  $m_t$  are hardly distinguishable. The reason is that using the ratio  $x/x_d$ , the residual  $m_t$  dependence is very mild. Our “best values” for the parameters  $(\rho, \eta)$ , together with the value of the CKM matrix element ratio  $|V_{td}/V_{ts}|^2$ ,

$m_t$ (GeV)	$(\rho, \eta)$	$ V_{td}/V_{ts} ^2$	$\chi^2_{\min}$
100	(0.01, 0.37)	0.056	0.03
140	(0.02, 0.34)	0.056	0.24
180	(0.03, 0.33)	0.057	0.93

Table 2: The “best values” of the CKM parameters  $(\rho, \eta)$  and the ratio  $|V_{td}/V_{ts}|^2$ , obtained by a minimum  $\chi^2$  fit of the experimental data discussed in the text, for 3 different values of  $m_t$ . Note that  $x_s = 15.0 \pm 3.0$  has been assumed for the fits. The resulting minimum  $\chi^2$  values from the MINUIT fits are also given.

and the  $\chi^2$  are given in Table 2. It is clear that the measurement of  $x_s$  would greatly help in reducing the uncertainty in the unitarity triangle. The CKM fits shown here can be repeated for other values of  $x_s$ , estimated in the standard model in the previous section.

### 3.4 Time-integrated measurements of $B^0$ - $\bar{B}^0$ Mixing – an update

We briefly discuss the present (time-integrated) measurements of  $B_s^0$ - $\bar{B}_s^0$  and  $B_d^0$ - $\bar{B}_d^0$  mixing. The data in the continuum have been analyzed in terms of the time-integrated quantity  $\chi$ , defined as:

$$\chi = P_d \chi_d + P_s \chi_s, \quad (38)$$

where  $P_d$  and  $P_s$  represent the probabilities  $P(b \rightarrow B_d)$  and  $P(b \rightarrow B_s)$ , respectively, and  $\chi_d$  and  $\chi_s$  are the  $B_s^0$ - $\bar{B}_s^0$  and  $B_d^0$ - $\bar{B}_d^0$  mixing parameters, defined in terms of the time-integrated probabilities:

$$\chi_{d,s} = \frac{P(B_{d,s} \rightarrow \bar{B}_{d,s}^0)}{P(B_{d,s} \rightarrow B_{d,s}) + P(B_{d,s} \rightarrow \bar{B}_{d,s}^0)}. \quad (39)$$

Note that  $\chi_{d,s}$  is related to  $x_{d,s}$  via

$$\chi_{d,s} = \frac{x_{d,s}^2}{2(1 + x_{d,s}^2)}. \quad (40)$$

The quantity  $\chi$  has been measured at LEP using the semileptonic decays of the  $B$ -hadrons, giving rise to the dilepton final states. It is easy to show that the following relation holds:

$$\frac{\Gamma(Z^0 \rightarrow b\bar{b} \rightarrow \ell^+ \ell^- X)}{\Gamma(Z^0 \rightarrow b\bar{b} \rightarrow \ell^+ \ell^- X)} = \frac{2\chi(1 - \chi)}{(1 - \chi)^2 + \chi^2}. \quad (41)$$

The present LEP-average is [14]:

$$\chi = 0.131 \pm 0.010. \quad (42)$$

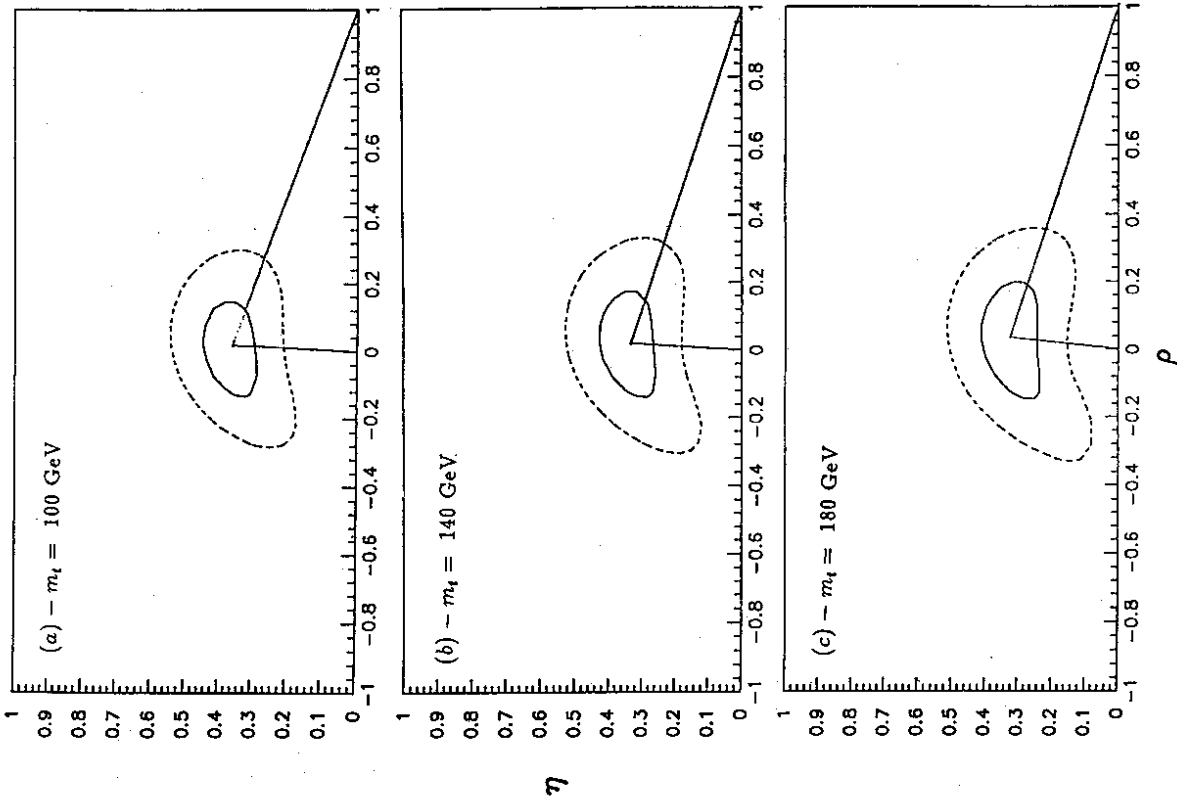


Figure 4: Allowed region in  $\rho$ - $\eta$  space for different values of the standard model parameters, assuming  $x_s = 15.0 \pm 3.0$ . Figs. (a)-(c) have  $m_t = 100, 140$  and  $180$  GeV, respectively. The solid line represents the region with  $\chi^2 = \chi^2_{\min} + 1$ ; the dashed line denotes the 90% c.l. region. The triangles show the best fit.

The measurements at the  $p\bar{p}$  colliders at CERN and Fermilab give [39,40]:

$$\begin{aligned}\chi &= 0.145 \pm 0.038 \quad (\text{UA1}), \\ \chi &= 0.176 \pm 0.050 \quad (\text{CDF}).\end{aligned}\quad (43)$$

To get an estimate of  $\chi$ , from the measured values of  $\chi$  and  $\chi_d$  (measured by the ARGUS and CLEO collaborations), one needs the value of the parameters  $f_d$  and  $f$ . Recently, first measurements of  $f$ , were presented from LEP using the production rate of  $B^0$  and  $b$ -baryons. Using the experimental value  $f$ , = 0.20 ± 0.07 and  $f_d$  = 0.35 ± 0.05, one can combine the LEP and ARGUS/CLEO measurements to give [14]:

$$\chi_s = 0.43 \pm 0.17, \quad (44)$$

in agreement with the large (almost complete) mixing anticipated for the  $B^0$ - $\bar{B}^0$  case in the standard model,  $\chi_s \simeq 0.50$ . However, it is clear that this measurement does not (yet) provide a stringent bound on the CKM matrix element  $|V_{cb}|$ . For example, at  $1\sigma$ , the measurement 44 translates into a bound  $x_s \geq 1.04$ , to be compared with the SM expectations estimated above, which are typically an order of magnitude higher.

More data at LEP would reduce the indicated errors on the quantities  $\chi$  and  $\chi_s$ . It is also important to think about measurements which could reduce the  $f$ , dependence. The first qualitative improvement at LEP is expected to come through time-integrated measurements of the final states in the decays  $Z^0 \rightarrow b\bar{b}$ , in which the quantity  $\chi$ , would be measured by invoking the characteristic flavour correlations due to  $B^0/\bar{B}^0$  production and decay [43]. A point in question is the measurement of the dilepton final state  $Z^0 \rightarrow b\bar{b} \rightarrow \ell^+\ell^-X$ , where now  $X$  includes a tagged  $D_s$ -meson. Since this ratio involves a different weighting of the quantities  $\chi_d$  and  $\chi_s$ , as compared to the dilepton ratio  $\chi$  without flavour tagging, defined earlier, the two measurements can be combined to extract  $\chi_s$ . The presence of the  $D_s$ -mesons in the decays of the  $B_s$  mesons has been gainfully used to detect the  $B_s$  meson and measure its lifetime at LEP [44]. The  $\ell^+\ell^-D_s^\pm$  states from  $B$  meson decays are anticipated to play a central role in the measurement of both the time-integrated quantity  $\chi_s$ , as well as the mixing ratio  $x_s$ . This and related correlations have been described in ref. [4], to which we refer for details.

## 4 CP Violation in the $B$ System

Mixing and CP violation in the  $B$  system can be described in much the same way as in the kaon system. In the  $B$  system, the states  $|B^0\rangle$  and  $|\bar{B}^0\rangle$  are eigenstates of the strong and electromagnetic interactions, but not of the weak interactions, which are responsible for their decay. Taking into account the weak interactions, one writes the  $2 \times 2$  Hamiltonian (in the  $B^0$ - $\bar{B}^0$  basis)

$$H = M - \frac{i}{2}\Gamma, \quad (45)$$

where the mass matrix  $M$  and the decay matrix  $\Gamma$  are Hermitian. (Since neutral  $B$ 's do decay,  $H$  itself is not Hermitian.) CPT invariance implies that the diagonal components of  $H$  are equal, and if CP is conserved,  $M$  and  $\Gamma$  are real. Allowing for the possibility of CP violation, diagonalizing the Hamiltonian

$$H = \begin{bmatrix} m & M_{12} \\ M_{12}^* & m \end{bmatrix} - \frac{i}{2} \begin{bmatrix} \Gamma_{12} & \\ & \Gamma \end{bmatrix} \quad (46)$$

yields the eigenstates  $B_L$  and  $B_H$  ( $L$  and  $H$  denote the light and heavy states, respectively):

$$\begin{aligned}|B_L\rangle &= p|B^0\rangle + q|\bar{B}^0\rangle, \\ |B_H\rangle &= p|B^0\rangle - q|\bar{B}^0\rangle,\end{aligned}\quad (47)$$

where

$$\frac{p}{q} = \frac{1 + \epsilon_B}{1 - \epsilon_B} = \sqrt{\frac{M_{12} - \frac{i}{2}\Gamma_{12}}{M_{12}^* - \frac{i}{2}\Gamma_{12}^*}}. \quad (48)$$

In Eq. 48, the symbol  $\epsilon_B$  has been introduced to indicate the relation between this notation and that used normally in the kaon system. Analogously to the kaon system, a nonzero value of  $\epsilon_B$  indicates CP violation in  $B^0$ - $\bar{B}^0$  mixing. However, there is a big difference in the  $B$  system – here it is found that  $|\epsilon_B| \ll |\epsilon_K|$  (recall that  $\Gamma_{12} \sim 2M_{12}$  for kaons). This implies that  $\epsilon_B$  is much smaller than  $\epsilon_K$ , so that prospects for the observation of CP violation in the  $\Delta B = 2$  transitions of  $B^0$ - $\bar{B}^0$  mixing are virtually hopeless. Luckily for us, CP violation in  $B$  decays ( $\Delta B = 1$ ) can be large. (This is another difference between the  $K$  and  $B$  systems – in the kaon system, CP violation in  $K$  decays ( $\epsilon'/\epsilon$ ) is small.) This can be seen explicitly by considering the time evolution of  $B$  mesons. Because of  $B^0$ - $\bar{B}^0$  mixing, a state which starts out as a pure  $B^0$  or  $\bar{B}^0$  will evolve in time to a mixture of  $B^0$  and  $\bar{B}^0$ :

$$\begin{aligned}|B^0(t)\rangle &= f_+(t)|B^0\rangle + \frac{q}{p}f_-(t)|\bar{B}^0\rangle \\ |\bar{B}^0(t)\rangle &= \frac{p}{q}f_-(t)|B^0\rangle + f_+(t)|\bar{B}^0\rangle.\end{aligned}\quad (49)$$

Here,  $|B^0\rangle$  represents a pure  $B^0$  state at  $t = 0$ ,  $|\bar{B}^0\rangle$  represents a pure  $\bar{B}^0$  state at  $t = 0$ , and

$$\begin{aligned}f_+(t) &= e^{-iMt}e^{-\Gamma t/2} \cos(\Delta Mt/2) \\ f_-(t) &= e^{-iMt}e^{-\Gamma t/2} i \sin(\Delta Mt/2),\end{aligned}\quad (50)$$

in which

$$M \equiv (M_H + M_L)/2, \quad \Delta M \equiv M_H - M_L. \quad (51)$$

The most promising signal of CP violation in  $B$  decays comes by considering a CP eigenstate final state  $f$  to which both  $B^0$  and  $\bar{B}^0$  can decay. CP violation is manifested in a non-zero value of [45]

$$A_f(t) = \frac{\Gamma(B^0(t) \rightarrow f) - \Gamma(\bar{B}^0(t) \rightarrow f)}{\Gamma(B^0(t) \rightarrow f) + \Gamma(\bar{B}^0(t) \rightarrow f)}. \quad (52)$$

The expression for this asymmetry can be calculated from Eqs. 49 and 50. It is

$$A_f(t) = -\text{Im} \alpha_f \sin x_q \frac{t}{\tau_B}, \quad (53)$$

in which  $x_q$ ,  $q = d, s$  is the  $B_q^0$ - $\bar{B}_q^0$  mixing parameter (Eqs. 17,30),  $\tau_B$  is the  $B$  lifetime, and

$$\alpha_f = \frac{q}{p} \rho_f, \quad (54)$$

where  $\rho_f$  is the ratio of the amplitudes for  $\bar{B}_q^0$  and  $B_q^0$  to decay to  $f$ ,

$$\rho_f = \frac{\langle f | H | \bar{B}_q^0 \rangle}{\langle f | H | B_q^0 \rangle}. \quad (55)$$

If all amplitudes which contribute to the decay  $B_q^0 \rightarrow f$  have the same CKM phase  $\phi_D$ , then  $\rho_f$  is a pure phase:

$$\rho_f = e^{-2i\phi_D}. \quad (56)$$

This is indeed the case, up to corrections from penguin diagrams [46], for all CP eigenstate final states. In addition, since  $\Gamma_{12} \ll M_{12}$ ,  $q/p$  is also a pure phase:

$$\frac{q}{p} = \sqrt{\frac{M_{12}^*}{M_{12}}} = e^{-2i\phi_M}. \quad (57)$$

Therefore

$$\alpha_f = e^{-2i(\phi_M + \phi_D)} \implies \text{Im} \alpha_f = -\sin 2(\phi_M + \phi_D). \quad (58)$$

Note that, although  $\phi_M$  and  $\phi_D$  each depend on the form chosen for the CKM matrix, the sum  $\phi_M + \phi_D$  is convention independent.

In the Wolfenstein parametrization (Eq. 1), only the matrix elements  $V_{cb}$  and  $V_{td}$  have large phases. In the following we will ignore all small CKM phases. It is not difficult to relate  $\phi_M$  and  $\phi_D$  to the CKM matrix elements. Like  $x_q$ ,  $M_{12}$  is calculable from the box diagram for  $B_q^0$ - $\bar{B}_q^0$  mixing (in fact,  $\Delta M = 2|M_{12}|$ ). Thus,  $M_{12} \sim (V_{cb} V_{td})^2$ , and therefore the phase information from the mixing is

$$\left(\frac{q}{p}\right)_{B_q} = \frac{V_{td}}{V_{td}^*}, \quad \left(\frac{q}{p}\right)_{B_s} = 1. \quad (59)$$

The phase information in the decay depends on whether the  $b$ -quark decays into a  $c$ - or a  $u$ -quark:

$$(\rho_f)_{b \rightarrow u} = \frac{V_{ub}}{V_{ub}^*}, \quad (\rho_f)_{b \rightarrow c} = 1. \quad (60)$$

There are therefore three classes of  $B$  decays into CP eigenstates which can have sizeable CP violating asymmetries. These are related to the three angles  $\alpha$ ,  $\beta$ ,  $\gamma$  of the unitary triangle (Fig. 1) as follows.

- $B_d$  decays with  $b \rightarrow c$ : For this class of decays, we have

$$\alpha_f = \frac{V_{td}}{V_{td}^*}, \quad \text{Im} \alpha_f = -\sin 2\beta. \quad (61)$$

The classic example here is  $B_d \rightarrow J/\Psi K_S$ . For this particular final state, since  $J/\Psi K_S$  is a CP-odd state, there is an additional minus sign in the asymmetry.

- $B_d$  decays with  $b \rightarrow u$ : Here we have

$$\alpha_f = \frac{V_{ub} V_{td}}{V_{ub}^* V_{td}^*}, \quad \text{Im} \alpha_f = \sin 2\alpha. \quad (62)$$

One example of such a decay is  $B_d \rightarrow \pi^+ \pi^-$ .

- $B_s$  decays with  $b \rightarrow u$ : In this case

$$\alpha_f = \frac{V_{ub}}{V_{ub}^*}, \quad \text{Im} \alpha_f = -\sin 2\gamma. \quad (63)$$

This angle is the most difficult to measure. One possible decay mode is  $B_s \rightarrow \rho K_S$ . Like the final state  $J/\Psi K_S$ ,  $\rho K_S$  is CP-odd, which changes the sign of the asymmetry.

The asymmetries in Eqs. 61,62 and 63 can be expressed straightforwardly in terms of the CKM parameters  $\rho$  and  $\eta$ . The 90% c.l. constraints on  $\rho$  and  $\eta$  found previously can be used to predict the ranges of  $\sin 2\alpha$ ,  $\sin 2\beta$  and  $\sin 2\gamma$  allowed in the standard model. The allowed ranges which correspond to each of the figures in Figs. 2 and 3 are found in Table 3. In this Table we have assumed that the angle  $\beta$  is measured in  $B_d \rightarrow J/\Psi K_S$ , and have therefore included the extra minus sign due to the CP of the final state.

Since the CP asymmetries all depend on  $\rho$  and  $\eta$ , the ranges for  $\sin 2\alpha$ ,  $\sin 2\beta$  and  $\sin 2\gamma$  shown in Table 3 are correlated. That is, not all values in the ranges are allowed simultaneously. We illustrate this in Figs. 5 and 6 by showing the region in  $\sin 2\alpha$ - $\sin 2\beta$  space allowed by the data, for various values of  $m_t$  and  $f_{B_d}^2 B_{B_d}$ . From these figures one sees that the smallest values of  $\sin 2\beta$  occur only in a small region of parameter space around  $\sin 2\alpha \simeq 0.2$ - $0.6$ . Excluding this small tail, one expects the CP-asymmetry in  $B_d \rightarrow J/\Psi K_S$  to be at least 30%, which is good news for  $B$ -factory proponents.

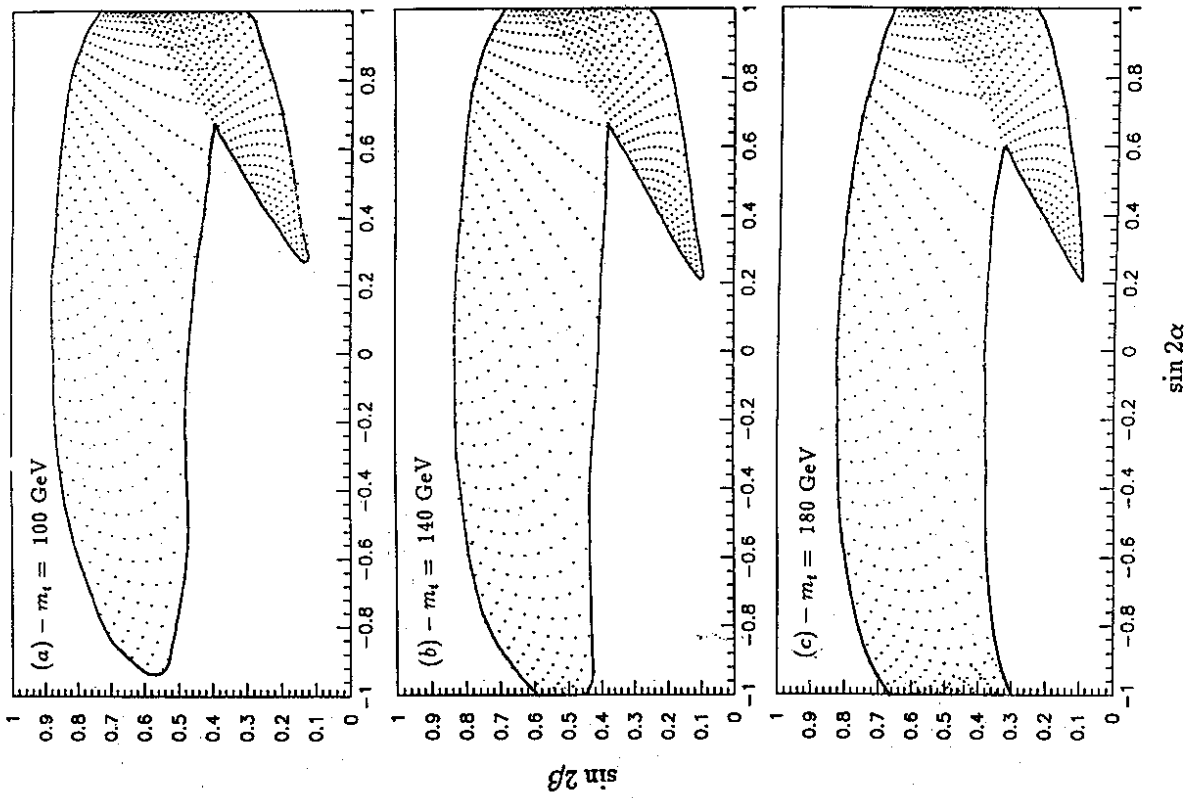


Figure 5: Allowed values of the CP asymmetries  $\sin 2\alpha$  and  $\sin 2\beta$  for different values of the standard model parameters. Figs. (a)-(c) have  $f_{B_d}\sqrt{B_{B_d}} = 135 \pm 25$  MeV, with  $m_t = 100$ , 140 and 180 GeV, respectively.

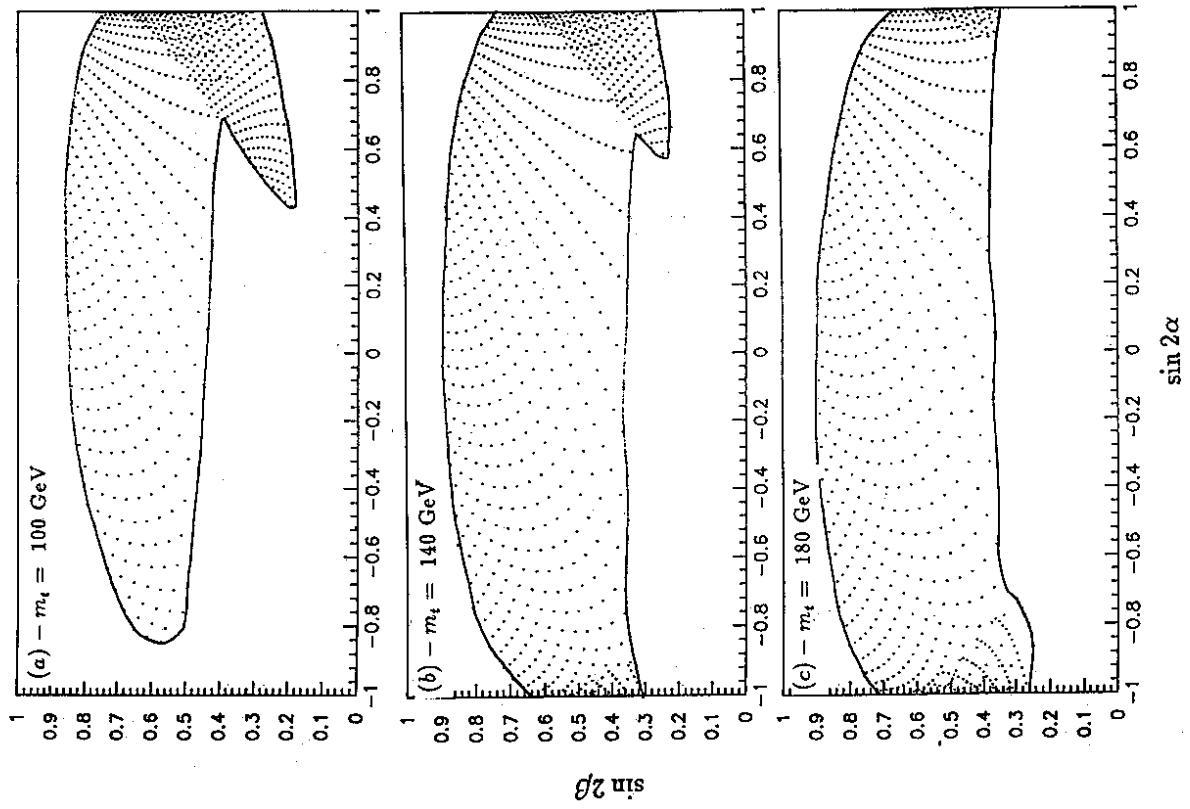


Figure 6: Allowed values of the CP asymmetries  $\sin 2\alpha$  and  $\sin 2\beta$  for different values of the standard model parameters. Figs. (a)-(c) have  $f_{B_d}\sqrt{B_{B_d}} = 200 \pm 30$  MeV, with  $m_t = 100$ , 140 and 180 GeV, respectively.

$m_t$ (GeV)	$f_{B_d}\sqrt{B_{B_d}}$ (MeV)	$\sin 2\alpha$	$\sin 2\beta$	$\sin 2\gamma$
100	$135 \pm 25$	$-0.93 - 1$	$0.12 - 0.87$	$-1 - 1$
140	$135 \pm 25$	$-1 - 1$	$0.09 - 0.83$	$-1 - 1$
180	$135 \pm 25$	$-1 - 1$	$0.10 - 0.82$	$-1 - 1$
100	$200 \pm 30$	$-0.85 - 1$	$0.18 - 0.86$	$-1 - 1$
140	$200 \pm 30$	$-1 - 1$	$0.22 - 0.89$	$-1 - 1$
180	$200 \pm 30$	$-1 - 1$	$0.25 - 0.89$	$-1 - 1$

Table 3: The allowed ranges for the CP asymmetries  $\sin 2\alpha$ ,  $\sin 2\beta$  and  $\sin 2\gamma$ , corresponding to the constraints on  $\rho$  and  $\eta$  shown in Figs. 2 and 3. Values of  $m_t$  and the coupling constant  $f_{B_d}\sqrt{B_{B_d}}$  are stated. The range for  $\sin 2\beta$  includes an additional minus sign due to the CP of the final state  $J/\Psi K_S$ .

## 5 Summary

One of the most important remaining tests of the standard model involves the precise determination of the CKM matrix parameters. The knowledge of the values of these parameters might give us some insight into the mechanism of symmetry breaking, particularly as regards the mass matrices. Furthermore, this information would allow us to ascertain whether the CKM matrix is the sole source of CP violation, or if new physics is needed.

Of the 4 CKM matrix parameters,  $\lambda$  is by far the most well-determined, having been accurately measured in  $\beta$  decay and in  $K \rightarrow \pi e \nu$  and hyperon decays:

$$\lambda = 0.2205 \pm 0.0018. \quad (64)$$

The extraction of  $|V_{cb}|$ , and hence  $A$ , from the semileptonic decays of  $B$  mesons has been greatly facilitated by the recent development of heavy-quark effective theory. With this tool, it has been found that

$$A = 0.90 \pm 0.12 \quad (65)$$

corresponding to

$$|V_{cb}| = 0.044 \pm 0.006. \quad (66)$$

The final two parameters of the CKM matrix,  $\rho$  and  $\eta$ , are somewhat constrained by the measurements of  $|\epsilon|$ ,  $x_d$  and  $|V_{cb}|/|V_{ub}|$ . We have fitted  $\rho$  and  $\eta$  to the data, taking the ranges of values for the hadronic matrix elements from lattice calculations:

$$\begin{aligned} B_K &= 0.8 \pm 0.2, \\ f_{B_d}\sqrt{B_{B_d}} &= 200 \pm 30 \text{ MeV}, \end{aligned} \quad (67)$$

although, for comparison, we have also used smaller values of  $f_{B_d}\sqrt{B_{B_d}}$ , typical of QCD sum rules and potential models:

$$f_{B_d}\sqrt{B_{B_d}} = 135 \pm 25 \text{ MeV}. \quad (68)$$

In addition, in the fits, we take three representative values of the top-quark mass,  $m_t = 100, 140$  and  $180$  GeV. We find that  $\eta$  is constrained to lie roughly in the range  $0.1-0.5$ , approximately independent of  $m_t$  and  $f_{B_d}\sqrt{B_{B_d}}$ . The range of  $\eta$  is due principally to the uncertainty in  $B_K$ . On the other hand,  $\rho$  is less well-determined. Its value lies between about  $-0.5$  and  $0.5$ , but depends strongly on  $m_t$  and  $f_{B_d}\sqrt{B_{B_d}}$ .

The measurement of  $x$ , would greatly help in constraining  $\rho$ , since its use would eliminate  $m_t$ -dependence and reduce the hadronic uncertainty. Using the above fits, the lower limit on  $x$ , is estimated to be (at “ $1\sigma$ ”):

$$\begin{aligned} x, &> 3.0 & (f_{B_d}\sqrt{B_{B_d}} &= 180 \pm 35 \text{ MeV}), \\ x, &> 5.2 & (f_{B_d}\sqrt{B_{B_d}} &= 225 \pm 25 \text{ MeV}). \end{aligned} \quad (69)$$

The corresponding “central values” (taking  $m_t = 150$  GeV) are

$$\begin{aligned} x, &= 10.0 & (f_{B_d}\sqrt{B_{B_d}} &= 180 \pm 35 \text{ MeV}), \\ x, &= 15.8 & (f_{B_d}\sqrt{B_{B_d}} &= 225 \pm 25 \text{ MeV}). \end{aligned} \quad (70)$$

To illustrate the importance of a measurement of  $x$ , in constraining the CKM matrix elements, we repeated the fits, assuming a hypothetical value for  $x$ , of  $15.0 \pm 3.0$ , and taking the current lattice calculation for the ratio of the hadronic uncertainties:

$$\frac{f_{B_d}^2 B_{B_d}}{f_{B_s}^2 B_{B_s}} = 1.19 \pm 0.10. \quad (71)$$

Although the range of  $\eta$  was not significantly altered,  $\rho$  was constrained to lie between  $-0.3$  and  $0.3$ , independently of  $m_t$ . This illustrates two important points. First of all, the measurement of  $x$ , will be very useful in determining the values of the CKM matrix parameters. Secondly, it is crucial that the lattice calculations of the hadronic matrix elements be as precise as possible. Reducing the errors on the lattice numbers will greatly help in ultimately pinning down the CKM parameters.

Finally, we used the current constraints on  $\rho$  and  $\eta$  to calculate the expected size of the CP-violating asymmetries in  $B$  decays. The quantities  $\sin 2\alpha$  and  $\sin 2\gamma$ , corresponding to CP asymmetries in  $B_d \rightarrow \pi^+ \pi^-$  and  $B_s \rightarrow \rho K_S$ , respectively, are completely unconstrained, their values lying anywhere between  $-1$  and  $1$ . On the other hand,  $\sin 2\beta$ , which signifies CP violation in the decay  $B_d \rightarrow J/\Psi K_S$ , is limited to be roughly in the range  $10-90\%$ , not a particularly stringent constraint. However, it must be noted that the smaller values of  $\sin 2\beta$  occur in a relatively small region of parameter space. If this region is excluded then this asymmetry is at least  $30\%$ .

## References

- [1] S.L. Glashow, Nucl. Phys. **22** (1961) 579; A. Salam in *Elementary Particle Theory*, ed. N. Svartholm (Almqvist and Wiksell, Stockholm, 1968); S. Weinberg, Phys. Rev. Lett. **19** (1967) 1264.
- [2] N. Cabibbo, Phys. Rev. Lett. **10** (1963) 531; M. Kobayashi and T. Maskawa, Prog. Theor. Phys. **49** (1973) 652.
- [3] L. Wolfenstein, Phys. Rev. Lett. **51** (1983) 1945.
- [4] A. Ali and D. London, DESY Report 075-92 (1992) (to be published in J. Phys. G: Nuclear and particle Physics, UK).
- [5] W.B. Atwood and J. Jaros, SLAC-PUB-5671 (1991) and in *B Physics*, ed. S. Stone (World Scientific, 1992).
- [6] M. Aguilar-Benitez et al. (Particle Data Group), Phys. Lett. **B239** (1990) 1.
- [7] S. Stone and H. Schröder (private communication).
- [8] A.J. Buras, M. Jamin and P.H. Weisz, Nucl. Phys. **B347** (1990) 491.
- [9] A.J. Buras, W. Slominski and H. Steger, Nucl. Phys. **B238** (1984) 529; **B245** (1984) 369.
- [10] N. Isgur and M. Wise, Phys. Lett. **B232** (1989) 113; **B237** (1990) 527.
- [11] M.E. Luke, Phys. Lett. **252B** (1990) 447.
- [12] C.G. Boyd and D.E. Brahm, Phys. Lett. **257B** (1991) 393.
- [13] M. Neubert and V. Rieckert, Nucl. Phys. **B38**: (1992) 97; M. Neubert, Phys. Lett. **264B** (1991) 455, Phys. Rev. **D46** (1992) 2212.
- [14] P.S. Drell and J. Ritchie Patterson, Cornell University Report CLNS-92-1177 (1992) (to appear in Proceedings of the XXVth. International Conference on High Energy Physics, Dallas, Texas, USA, (1992)).
- [15] H. Albrecht et al. (ARGUS Collaboration), DESY 92-146 (1992).
- [16] G. Altarelli, M. Cabibbo, G. Corbo, L. Maiani and G. Martinelli, Nucl. Phys. **B208** (1982) 365.
- [17] J. Flynn, Mod. Phys. Lett. **A5** (1990) 877.
- [18] T. Inami and C.S. Lim, Prog. Theor. Phys. **65** (1981) 297.
- [19] F. Abe et al. (CDF), Phys. Rev. **D45** (3921) (1992).
- [20] G. Altarelli, CERN-TH.6206/91 (1991).
- [21] J. Ellis, G.L. Fogli and E. Lisi, Phys. Lett. **B274** (1992) 456.
- [22] P. Langacker and M. Luo, Phys. Rev. **D44** (1991) 817.
- [23] R. Tanaka, Ecole Polytechnique, IN2P3-CNRS Report X-LPNHE/92-3 (1992) (to appear in Proceedings of the XXVth. International Conference on High Energy Physics, Dallas, Texas, USA, (1992)).
- [24] M. Danilov, Proceedings of the *International Lepton-Photon Symposium and Europhysics Conference on High Energy Physics*, S. Hegerty, K. Potter and E. Quercigh eds. (Geneva, 1991).
- [25] G. Martinelli (these proceedings).
- [26] C. Sachrajda, invited talk at the Conference: QCD-20 Years Later, Aachen, June 9-13 (1992).
- [27] M. Schmidtler and K.R. Schubert, Z. Phys. **C53** (1992) 347; A. J. Buras and M.K. Harlander, MPI-PAE/PTh 1/92, TUM-T31-25/92, and in *Heavy Flavours* eds. A.J. Buras and M. Lindner (World Scientific, Singapore, 1992).
- [28] S. Aoki et al. (WA75 Collaboration), CERN-PPE/92-157 (to appear in Prog. Theor. Phys.).
- [29] S. R. Sharpe, Nucl. Phys. **B17** (Proc. Supp.) (1990) 155.
- [30] For a review, see I. Bigi, V. Khoze, N. Uraltsev, and A. Sanda, in *CP Violation*, ed. C. Jarlskog (World Scientific) (1989) 175, and references quoted therein.
- [31] R. Aleksan et al. (these proceedings).
- [32] For a review, see I. Dunitz, in *B-Decays*, ed. S. Stone (World Scientific) 1992, and references quoted therein.
- [33] A. Ali, C. Greub and T. Mannel (these proceedings).
- [34] A. Ali, DESY Report 91-080 (1991) and in *Proc. of First Int. A.D. Sakharov Conf. on Physics, Lebedev Inst., Moscow* (1991).
- [35] C. Alexandrou et al., Nucl. Phys. **B374** (1992) 263.
- [36] A. Abada et al., Nucl. Phys. **B376** (1992) 172.

- [37] O. Pene, talk at the ECFA B Workshop, DESY, October 1992.
- [38] R.A. Bertlman and A. Martin, Nucl. Phys. **B168** (1980) 111; N. Byers and D.S. Hwang, in *Proceedings of the Workshop on High Sensitivity Beauty Physics at Fermilab*, Batavia, Illinois, 1987, edited by A.J. Slaughter, N. Lockyer, and M. Schmidt (Fermilab, Batavia, 1987), p. 199; A. Martin and J.M. Richard, Phys. Lett. **B185** (1987) 426; W. Kwong and J.L. Rosner, Phys. Rev. **D44** (1991) 212.
- [39] C. Albajar et al. (UA1), Phys. Lett. **B262** (1991) 171.
- [40] F. Abe et al. (CDF), Phys. Rev. Lett. **24** (1991) 3351.
- [41] D. Brown (ALEPH), Parallel session talk, LP-HEP 91, Geneva, Switzerland.
- [42] H. Schröder, DESY 91-139, and in *B Decays* ed. S. Stone, World Scientific (1992).
- [43] A. Ali and F. Barreiro, Z. Phys. **C30**(1986) 635.
- [44] P. Abreu et al. (DELPHI), Phys. Lett. **B289** (1992) 199. D. Buksulic et al. (ALEPH), Phys. Lett. **B294** (1992) 145. P.D. Acton et al. (OPAL), Phys. Lett. **B295** (1992) 357.
- [45] A. Carter and A. I. Sanda, Phys. Rev. Lett. **45** (1980) 952; Phys. Rev. **D23** (1981) 1567; I. I. Bigi and A. I. Sanda, Nucl. Phys. **B193** (1981) 85; **B281** (1987) 41; Y. Azimov, V. Khoze, and M. Uraltsev, Yad. Fiz. **45** (1987) 1412; D. Du, I. Dunietz, and D. Wu, Phys. Rev. **D34** (1986) 3414.
- [46] M. Gronau, Phys. Rev. Lett. **63** (1989) 1451; D. London and R.D. Peccei, Phys. Lett. **B223** (1989) 257; B. Grinstein, Phys. Lett. **B229** (1989) 280.